# pH-responsive IPN beads of carboxymethyl konjac glucomannan and sodium carboxymethyl cellulose as a controlled release carrier for ibuprofen

Alka Lohani [a,*], Ritika Saxena [b], Shahbaz Khan [b], Filipa Mascarenhas-Melo [c,d,**]

[a] Amity Institute of Pharmacy, Amity University Uttar Pradesh, Noida 201313, India
[b] Pharmacy Academy, IFTM University, Moradabad, Uttar Pradesh 244102, India
[c] Higher School of Health, Polytechnic Institute of Guarda, Rua da Cadeia, 6300-307 Guarda, Portugal
[d] REQUIMTE/LAQV, Department of Pharmaceutical Technology, Faculty of Pharmacy, University of Coimbra, Azinhaga de Santa Comba, 3000-548 Coimbra, Portugal

A B S T R A C T

The convergence of polymer and pharmaceutical sciences has advanced drug delivery systems significantly. Carbohydrate polymers, especially carboxymethylated ones, offer versatile benefits for pharmaceuticals. Interpenetrating polymer networks (IPNs) combine synthetic and natural polymers to enhance drug delivery. The study aims to develop IPN beads using sodium carboxymethyl cellulose (SCMC) and carboxymethyl konjac glucomannan (CMKGM) for controlled release of ibuprofen (IB) after oral administration. Objectives include formulation optimization, characterization of physicochemical properties, evaluation of pH-dependent swelling and drug release behaviors to advance biocompatible and efficient oral drug delivery systems. The beads were analyzed using SEM, FTIR, DSC, and XRD techniques. Different ratio of polymers (CMKGM:SCMS) and crosslinker concentrations (2&4 %w/v) were used, significantly impacting bead size, swelling, drug encapsulation, and release characteristics. DSC results indicated higher thermal stability in IPN beads compared to native polymers. XRD revealed IB dispersion within the polymer matrix. IPN beads size ranged from $580 \pm 0.56$ to $324 \pm 0.27$ μm, with a nearly spherical shape. IPN beads exhibited continuous release in alkaline conditions (pH 7.4) and minimal release in acidic media (pH 1.2). These findings suggest that the formulated IPN beads can modulate drug release in both acidic and alkaline environments, potentially mitigating the gastric adverse effects often associated with oral administration of IB.

## 1. Introduction

Over the last few decades, polymers, renowned for their remarkable adaptability, have revolutionized various aspects of our daily existence. Notably, the convergence of polymer science with pharmaceutical sciences has yielded significant advancements in the realm of drug delivery systems. This synergy has led to unprecedented levels of novelty, characterized by enhanced flexibility in terms of physical state, form, size, and surface properties of drug carriers [1]. This collaborative effort has propelled the evolution of polymers toward the creation of innovative biomaterials tailored specifically for controlled drug delivery applications [2]. These novel biomaterials exhibit sophisticated characteristics that enable precise modulation of drug release kinetics, targeting specific tissues or cells, and minimizing adverse effects. Such advancements

hold promise for addressing complex therapeutic challenges and improving patient outcomes across diverse medical domains [3–5].

Among these innovative materials, carbohydrate polymers stand out as a promising class of materials for drug delivery applications, offering a wide range of benefits and opportunities for innovation in the development of advanced therapeutic formulations [6]. The objective of carboxymethylation of carbohydrate polymers is to enhance their solubility and hydrophilicity, which improves their ability to form stable gels. Carboxymethylation of carbohydrate polymers represents a significant avenue in drug delivery research, offering versatile benefits for tailored pharmaceutical applications. In this chemical modification method, the backbone of the carbohydrate polymer is modified by adding carboxymethyl groups. Carboxymethylation of carbohydrate polymers offers a promising approach for enhancing the performance

---

\* Corresponding author.
\*\* Correspondence to: F. Mascarenhas-Melo, Higher School of Health, Polytechnic Institute of Guarda, Rua da Cadeia, 6300-307 Guarda, Portugal.
E-mail addresses: alohani@amity.edu (A. Lohani), filipamelo@ff.uc.pt (F. Mascarenhas-Melo).

and functionality of drug delivery systems [7]. Through the incorporation of carboxymethylated carbohydrate polymers, researchers can tailor drug delivery carriers to achieve desired properties such as improved solubility, mucoadhesion, pH responsiveness, and targeted drug release, thereby advancing the development of effective pharmaceutical formulations [8].

Interpenetrating polymer networks (IPNs) emerge as a novel category of polymers, hybridizing synthetic and/or natural polymers either independently or in combinations. IPNs offer a platform for designing drug delivery systems with tailored properties, combining the favorable attributes of different polymers to achieve enhanced performance and functionality. The use of IPN beads as a dosage form offers a multitude of advantages that can improve the effectiveness and safety of drug therapies. Their ability to provide controlled and sustained release, enhance drug stability and bioavailability, and enable targeted delivery makes them a valuable tool in modern pharmaceutics [9,10]. Although there are other delivery systems described in the literature, we highlight IPN beads due to their outstanding characteristics and specific applications. Although these systems may also have limitations, Table 2 summarizes the main characteristics associated with IPNs, providing a comparative analysis.

A water-soluble dietary fiber named konjac glucomannan (KGM) originates from the roots of the konjac plant, *Amorphophallus konjac*, indigenous to Southeast Asia [11]. KGM is well known for its special qualities and wide range of uses in the food and beverage cosmetic, and pharmaceutical sectors. KGM is typically classified as a high molecular weight polysaccharide ranging from 200 to 2000 kDa, and offers commendable biocompatibility and biodegradability [12]. However, this high molecular weight imposes limitations on its versatility in various applications. The biological activity of KGM varies significantly depending on its molecular weight, with lower molecular weights generally associated with higher activity levels [13]. Carboxymethylation is a widely used method for altering the charge characteristics of polysaccharides [14]. The hydroxyl groups on KGM's molecular chains serve as active sites, pivotal for extending its usefulness and enabling new functionalities. Carboxymethylation of KGM led to a reduction in the molecular weight and viscoelastic properties while enhancing the thermal stability and water solubility of KGM [14]. Therefore, carboxymethylation of KGM expands its utility and enhances its performance in diverse applications, offering valuable opportunities for innovation in the pharmaceutical, food, and industrial sectors [15]. KGM is a biopolymer but after chemical modification, we got CMKGM which will be a semi-synthetic polymer. Carboxymethylation of KGM was done to enhance the compatibility and interfacial adhesion between the fibers. This modification improves the dispersibility of the CMKGM within the polymer matrix, leading to enhanced mechanical properties and structural integrity of the composite beads.

Another polymer used in the study is SCMC, which is highly water-soluble and biocompatible, making it suitable for various biomedical and pharmaceutical applications. SCMC is considered a modified biopolymer rather than a purely natural biopolymer or synthetic polymer. It is derived from cellulose, a natural polymer found in the cell walls of plants, which makes it biodegradable and derived from renewable resources. Its ability to form hydrogels is beneficial for IPN systems that require a matrix capable of interacting with water or biological fluids. The selection of SCMC for IPN formation is based on its favorable properties, including water solubility, biocompatibility, hydrogel-forming ability, viscosity modulation, chemical reactivity, non-toxicity, biodegradability, and compatibility with other polymers [16–18].

Ibuprofen (IB), a nonsteroidal anti-inflammatory drug, was chosen as the model drug in this research. IB is commonly used to alleviate pain and inflammation associated with musculoskeletal disorders and other painful conditions [19]. However, it poses challenges due to its low water solubility and short plasma half-life of 1–3 h after oral administration [20], necessitating frequent dosing to sustain desired levels.

Additionally, its potential gastrointestinal side effects, ranging from mild discomfort to gastric bleeding, make it an excellent candidate for developing controlled-release formulations [21].

The aim of this study is the formulation of IPN beads using CMKGM and SCMC for the oral delivery of Ibuprofen (IB). By formulating these IPN beads through ionic gelation with AlCl₃ as a crosslinking agent, the research aims to achieve precise control over IB release specifically in the intestine to overcome the gastric side effects. The key objectives include formulation optimization, characterization of physicochemical properties, and evaluation of pH-dependent swelling and *in vitro* drug release behavior, aiming to advance biocompatible and efficient drug delivery systems. Additionally, the study investigates the influence of formulation parameters such as the CMKGM to SCMC ratio and AlCl₃ concentration on the physical and chemical properties of the IPN beads.

## 2. Materials and methods

### 2.1. Materials

Ibuprofen was sourced from Yarrow Chemical Products, located in Mumbai, India. KGM was acquired as a complimentary sample from Sarda Bio Polymers Private Limited, situated in Rajasthan, India, is a water-soluble dietary fiber known for its high molecular weight (200–2000 kDa), biocompatibility, and biodegradability. Concentrated hydrochloric acid, aluminium chloride, sodium carboxymethyl cellulose were bought from Central Drug House (P) LTD, a company located in New Delhi. HCl was used for adjusting pH, AlCl₃ as a crosslinking agent, and SCMC as a component of the IPN beads. Monochloroacetic acid (MCA) and methanol were supplied by Himedia Laboratories (P) LTD, headquartered in Mumbai. MCA was used in the carboxymethylation process of KGM, while methanol served as a solvent. All additional reagents obtained were of analytical grade.

### 2.2. Carboxymethylation of Konjac glucomannan (KGM)

Carboxymethylation serves as a widely employed method to alter the charge characteristics of polysaccharides. The synthesis of the CMKGM was carried out by the following procedure with little modification [31]. 2 g of KGM was dissolved in a mixture of aqueous methanol (30:70 ratio) containing 0.100–0.175 mol of sodium hydroxide (NaOH) at 300 °C with vigorous stirring (500 rpm) for 15 min at (in presence of NaOH, the pH of the solution rise sharply. The target pH is generally between 12 and 14. This highly alkaline environment is necessary to deprotonate the hydroxyl groups on the KGM, making them more reactive toward the chloroacetic acid during the carboxymethylation reaction). Subsequently, 0.042–0.095 mol of monochloroacetic acid (MCA) were introduced, and the blend was allowed to react at 50 °C for 180 min under reflux conditions. The product was filtered (Whatman Grade 3) and neutralized with diluted hydrochloric acid (1:1 *v/v*) once the reaction was finished. After adding methanol to the resultant solution, the precipitated mass was rinsed twice or three times with aqueous methanol. To produce CMKGM, it was then dried overnight at 45 °C in a vacuum oven. Fig. 1 shows the schematic representation of the carboxymethylation process.

### 2.3. Characterization of CMKGM

#### 2.3.1. Degree of substitution

500 mg of CMKGM was accurately weighed and dispersed in 5 ml of 80 % methanol. A small amount of concentrated HCl was added and stirred for a duration of 2 to 3 h. Whatman filter paper (WHA111703, Sigma-Aldrich Chemicals Private Limited, Bangalore, India) was used to filter the mixture. Following that, 5 ml of methanol washes were employed to rinse the residue until the washings reached a neutral pH, and then dried until a consistent weight was achieved. In an Erlenmeyer flask, 200 mg of the dried material was meticulously weighed. The liquid
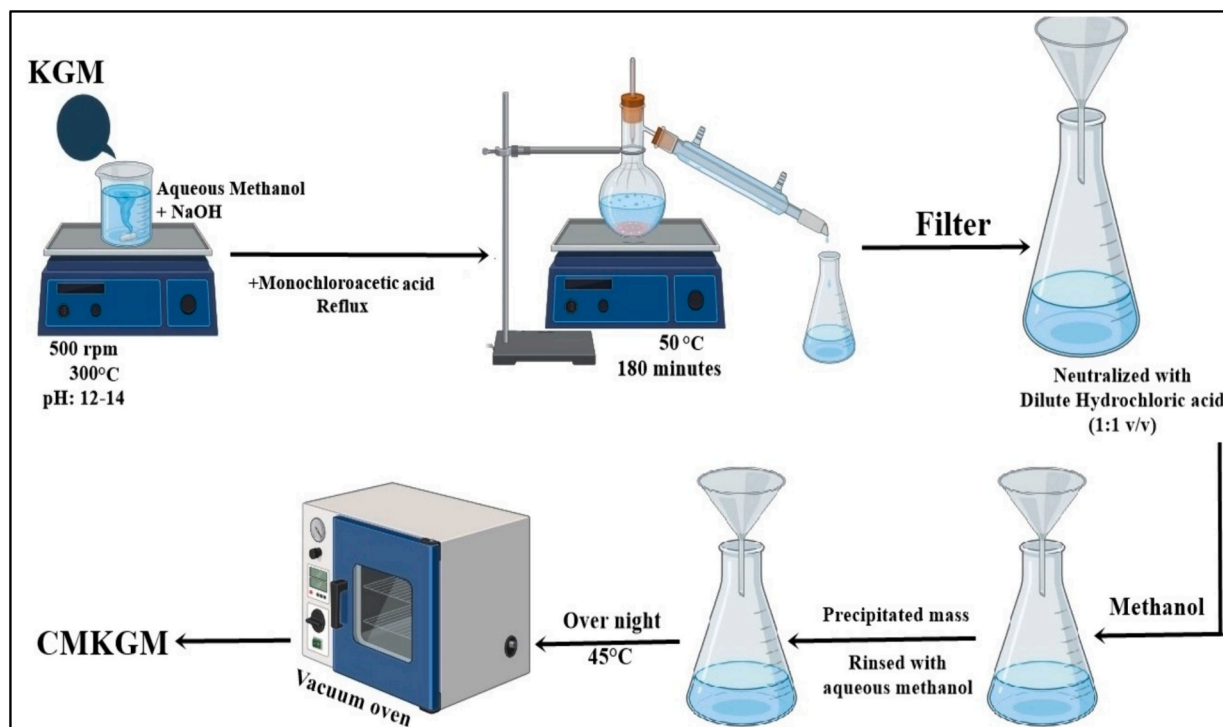
**Fig. 1.** Schematic representation of the carboxymethylation process.

mixture was allowed to stand for a short period of time following the addition of 1.5 ml of methanol (70 %). The mixture was then combined with water (20 ml) and sodium hydroxide (5 ml;0.5 N). The sample was stirred for 2 to 3 h for it to dissolve entirely. After that, the solution was once more titrated to a phenolphthalein end-point using hydrochloric acid (0.4 N) [14].

### 2.3.2. Fourier transform infrared spectroscopy

The Shimadzu FTIR spectrophotometer was utilized to analyze the FTIR spectra of KGM and CMKGM to assess the efficacy of carboxymethylation or the incorporation of carboxyl groups into the polymer (KGM) backbone. The FTIR spectra of pure IB and the physical mixture consisting of polymers (CMKGM & SCMC) and IB, were analyzed employing the KBr pellet approach. This will ensure any possible interaction between the drug and polymers. The samples were finely ground and mixed with potassium bromide (KBr) in a ratio of approximately 1:100 (sample). The mixture was then compressed under high pressure to form a transparent pellet suitable for FTIR analysis. The prepared KBr pellets were placed in the sample holder of the Shimadzu FTIR spectrophotometer. FTIR spectra were recorded in the range of 4000–400 cm$^{-1}$.

### 2.3.3. $^{13}C$ NMR Spectroscopy

The native KGM and CMKGM powders were separately suspended in deuterium oxide (D$_2$O) and left overnight and ensured the sample was fully dissolved to obtain clear and interpretable spectra, which were then transferred to 5 mm NMR tubes and subjected to $^{13}C$ NMR spectrum recording with NMR spectrometer (Bruker Avance Neo 500 MHz NMR Spectrometer) at 500 MHz. The following spectrometer parameters were used to record spectra- Frequency: 125.767 MHz; LB -1.00 Hz; PC-1.40 [32,33].

### 2.4. Preparation of IPN beads

To fabricate IPN beads containing IB the ionic gelation method was employed utilizing AlCl$_3$ as the cross-linking agent. A precisely

measured amount of IB was incorporated into an aqueous solution containing both CMKGM and SCMC, ensuring thorough mixing to achieve homogeneity. Next, a hypodermic needle (21-gauge) was used to progressively introduce drops of this dispersion into a mildly agitated AlCl$_3$ aqueous solution. An automated dispensing system was employed to ensure a consistent flow rate and pressure during bead formation. The resulting IB-loaded beads were immersed in the AlCl$_3$ solution and left for 30 min (gelation time). Following this, the beads were gently removed and subjected to repeated washing with distilled water (2–3 times) to eliminate any residual unreacted ions. Subsequently, they were allowed to dry (45 °C) until completely devoid of moisture. To preserve and stabilize the dried IPN beads until they were used again, they were kept in a vacuum desiccator [34]. The schematic representation and formulation composition of IPN beads are presented in Fig. 2 and Table 1, respectively.

### 2.5. Formation of IPN beads

IPN beads for oral delivery of IB were successfully prepared. In our study, the production of IPN beads was meticulously optimized by evaluating several critical factors to achieve beads with desirable mechanical properties, drug encapsulation efficiency, and controlled release profiles. The following factors were taken into account while producing the IPN beads:

1- Polymeric blend concentration remained constant (3 % *w/v*). Our preliminary trial studies led us to conclude that decreasing the concentration below 3 % w/v resulted in significantly weakened bead strength (loss of structural integrity). On the other hand, concentrations exceeding 3 % w/v resulted in polymer gels too thick to be effectively dispensed from the syringe. During the preliminary trials to check the bead strength, beads were placed between two fingers and compressed. It was observed that beads formed at 3 % *w/v* concentration showed the highest resistance to deformation, indicating superior compressive strength compared to beads at lower (1 % and 2 %).
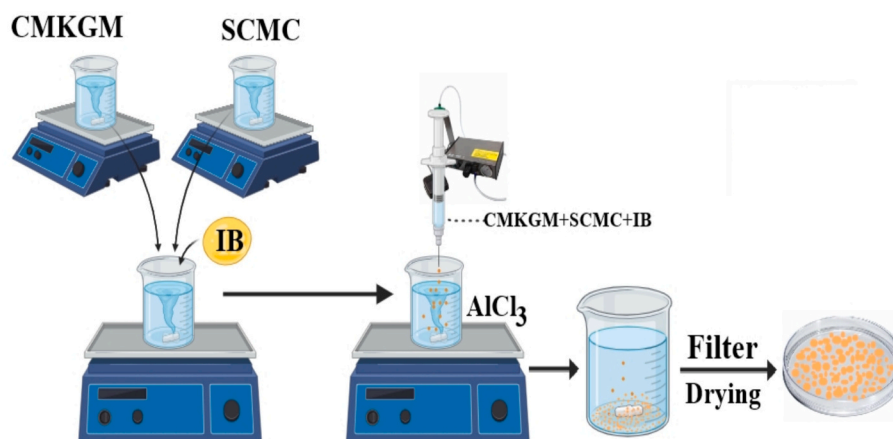
**Fig. 2.** Schematic representation of IPN bead formulation.

**Table 1**
IB-loaded IPN beads formulation composition.

| Formulation | CMKGM: SCMC (%w/v) | Loading of Drug* (%w/w) | AlCl₃ (%w/v) |
|---|---|---|---|
| $F_1$ | 1:1 | 30 | 2 % |
| $F_2$ | 1.5:1 | 30 | 2 % |
| $F_3$ | 2:1 | 30 | 2 % |
| $F_4$ | 1:1.5 | 30 | 2 % |
| $F_5$ | 1:2 | 30 | 2 % |
| $F_6$ | 1:1 | 30 | 4 % |
| $F_7$ | 1.5:1 | 30 | 4 % |
| $F_8$ | 2:1 | 30 | 4 % |
| $F_9$ | 1:1.5 | 30 | 4 % |
| $F_{10}$ | 1:2 | 30 | 4 % |

* (% w/w of total polymer).

2- The ratio of CMKGM to SCMC was varied to investigate the influence of each polymer individually.

3- During preliminary trials, it was determined that the optimal concentration range of $AlCl_3$ for producing robust, spherical, and easily separable beads fell between 2 % - 4 % w/v. Beads formed with $AlCl_3$ concentrations within this range exhibited sufficient mechanical strength to withstand handling stresses (slow agitation of crosslinker solution during gelation, filtration, drying) without breaking or deforming. The beads were observed for their ability to settle uniformly in a solution and their ease of filtration from the solution. Beads that clump together or have irregular shapes are more difficult to separate. The beads were manually handled to evaluate how easily they could be separated without sticking together or breaking.

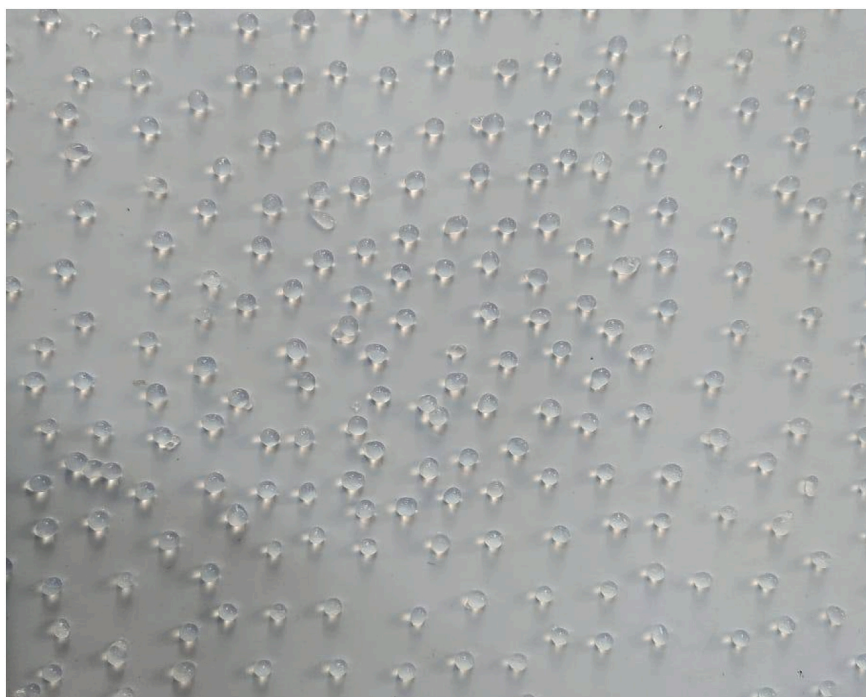Fig. 3 shows the beads after taking out from the crosslinking solution.



**Fig. 3.** Prepared IPN beads after separation from $AlCl_3$.

## 2.6. Characterization of IPN beads

### 2.6.1. Differential scanning calorimetry

The DSC thermograms of IB, unloaded IPN beads, and IB-loaded beads were carried out by using Differential Scanning Calorimeter (Make-Setaram; model: setline DSC+). A carefully weighed (2 mg) sample was stored in an aluminium pan that was hermetically sealed. The measurements were performed in a nitrogen atmosphere (20 ml/min), the heating rate was 10.00 °C/min and temperatures ranged from 20.00 °C to 440.00 °C [35].

### 2.6.2. X-ray diffraction studies

IB, blank IPN beads, and IB-loaded IPN beads were scanned using an X-ray diffractometer (D8 advance Plus, Bruker, U.S.) under the following circumstances. A diffraction angle of 2θ was used to scan the various samples, and a temperature range of 0 to 50 °C was covered. This was accomplished using a Ni-filtered Cu-Kα (λ = 1.54) radiation source with 30 mA of current and 40 kV of voltage supplied. The scanning speed that was employed was five degrees per minute.

### 2.6.3. Estimation of percentage yield

The percentage yield for various IPN bead compositions was determined by dividing the total amount of prepared IPN beads by the total amount of polymers and IB used during the manufacturing process. It was calculated by using the following formula (Formula (1)) [34]:

$$\text{Percentage yield (\%)} = \frac{\text{Total amount of prepared beads}}{\text{Amount of drug} + \text{total amount of polymers}} \times 100 \tag{1}$$

### 2.6.4. IPN bead size analysis

The size of IB-loaded IPN beads was measured with an optical microscope. To calibrate the ocular micrometer, a conventional stage micrometer was used. The divisions of the calibrated eyepiece were measured and beads were placed to a glass slide. The calibrated eyepiece micrometer was used to measure the diameter of each individual bead. 500 beads were measured and mean diameter was calculated. The Formula (2) was used to determine the diameter of each individual particle [35]:

### 2.6.5. Determination of drug encapsulation efficiency

Dried IPN beads (10 mg) were pulverized using a mortar and pestle, and then immersed in 10 ml of methanol. Following a 12-hour period, the suspension underwent filtration, and samples were scrutinized utilizing a UV–Visible spectrophotometer at 223 nm. This experiment was repeated thrice for validation. The DEE (%) was determined using the equation (Formula (3)) [34]:

$$\text{Drug Encapsulation Efficiency (\%)} = \frac{\text{Experimental drug content}}{\text{Theoretical drug content}} \times 100 \tag{3}$$

### 2.6.6. Swelling response to different pH

The swelling capacity of IB-loaded IPN beads from all batches was investigated in aqueous solutions with pH 1.2, 3.0, 6.5, 7.4, 9.0. 50 mg of IPN beads were taken in petri dishes containing 10 ml of the respective acidic or alkaline media of different pH. At an interval of 1 h up to 24 h, the beads were removed, excess surface water was gently blotted off, and the swollen beads were weighed to calculate the swelling ratios [36,37]. All measurements were performed in triplicate. In order to obtain the results the following formula (Formula (4)) was applied:

$$\text{\%equilibrium water uptake} = \frac{(\text{mass of swollen beads} - \text{mass of dried beads})}{\text{mass of dried beads}} \times 100 \tag{4}$$

### 2.6.7. Surface morphology of IPN beads

SEM analysis was performed in order to obtain topographical information about the beads. The Nova Nano FEG-SEM 450 a high-resolution scanning electron microscope was used to measure the exterior morphology of placebo and drug-loaded beads. SEM images of uncoated beads were acquired at 1.0 mmHg of chamber pressure and an acceleration voltage of 17 kV [38].

## 2.7. Drug release from IPN beads, kinetics and mechanism

For the *in-vitro* release study of IB, a dissolution apparatus of the Basket type (USP Apparatus-I) was utilized. The release of IB was assessed in gastric contents, first at pH 1.2 for the first 2 h and then at pH 7.4 to mimic gastric and intestinal conditions. Accurately weighed IB-loaded dried IPN beads, equivalent to 100 mg of the drug, were placed in 900 ml of dissolution media maintained at 37 ± 0.5 °C. The basket was rotated at 50 rpm. At regular intervals, 5 ml sample was withdrawn (at 1 h intervals) and replaced immediately with the same volume of fresh dissolution medium. The withdrawn samples were analyzed using UV–Visible spectrophotometer at 223 nm. We used a variety of empirical equations, such as zero, first order, Korsmeyer-Peppas, and Higuchi models, to study the kinetics of drug release.

## 3. Results and discussion

In this section, we have presented the outcomes of our study on the characterization of carboxymethylation of KGM, and the characterization of IPN beads. The results highlight key findings regarding bead

$$1 \text{ eyepiece micrometer division} = \frac{\text{Number of stage micrometer division}}{\text{Number of eyepiece micrometer division}} \times 100 \tag{2}$$

morphology, IB encapsulation efficiency, swelling behavior, and *in-vitro* drug release studies. Additionally, the discussion delves into the influence of formulation parameters such as CMKGM to SCMC ratio and AlCl$_3$ concentration on these properties, aiming to optimize the performance of IPN beads as effective drug delivery carriers. Table 2 summarizes the specific advantages and potential limitations of this study in comparison with the general results obtained in other studies.

## 3.1. Carboxymethylation of Konjac Glucomannan

The carboxymethylation of KGM was done. Fig. 4 shows the images

**Table 2**

Advantages and limitations of IPN systems: general considerations and specific considerations of this study.

| Aspect | General advantages | Advantages of this study | General limitations | Disadvantages of this study | Reference |
|---|---|---|---|---|---|
| Mechanical Properties | Enhanced mechanical strength and elasticity | Improved strength due to the interpenetrating network of CMKGM and SCMC | Synthesis of IPN beads can be complex and time-consuming | Synthesis complexity and time consumption. However, the resulting benefits and unique properties make them a valuable focus of study | [20,22] |
| Controlled Drug Release | More controlled and sustained drug release profiles | pH-responsive release of Ibuprofen, allowing for targeted and controlled oral drug delivery | Sometimes the polymers interpenetrate so extensively that releasing the active drug from the polymer matrix becomes challenging | There might be some possibility that releasing the drug from the highly interpenetrated network could be challenging | [9,23] |
| Swelling Behavior | Improved swelling properties | Analyzing the swelling behavior of the IPN beads in this study provided several critical advantages: - understanding pH-responsive behavior; - controlled drug release; - effectiveness of beads for oral drug delivery | Variations in polymer properties and synthesis conditions can lead to inconsistencies | Potential instability was observed at higher pH | [24,25] |
| Stimuli Sensitivity | Sensitivity to stimuli like pH and temperature makes them unique | pH-responsive behavior enables controlled release in specific gastrointestinal regions after oral administration | Potential instability under fluctuating environmental conditions | Stability of pH-responsive behavior under different physiological conditions may vary | [26] |
| Biocompatibility | Reduced risk of adverse reactions with biocompatible polymers | Enhanced biocompatibility with the use of natural polysaccharides like KGM and SCMC | Finding compatible polymers that can form a stable interpenetrating network while maintaining desirable properties can be restrictive | Biocompatibility in long-term applications needs further study | [27] |
| Versatility in drug selection and formulation | Ability to incorporate a wide range of drugs, including hydrophilic and hydrophobic drugs and ability to prepare a wide range of delivery systems, including beads, microspheres, nanoparticles, membranes, *etc*. | Effective encapsulation and release of Ibuprofen, demonstrating the potential for other drugs for oral controlled drug delivery | Scalability issues from laboratory to industrial scale | Scalability from laboratory synthesis to industrial production remains a challenge | [28–30] |



**Fig. 4.** CMKGM before and after drying.

of CMKGM before and after the drying of the carboxymethylation process.

### 3.1.1. Characterization of Carboxymethyl Konjac Glucomannan

*Degree of substitution:* The degree of substitution (DoS) plays a crucial role, particularly in determining various characteristics such as emulsifiability, solubility, stability, thickening properties, acid resistance, and salt tolerance. It quantifies the number of hydrogens in the hydroxyl group of the glucose unit replaced by carboxymethyl [37]. From the results obtained, the DoS of CMKGM, was found to be 1.6. The DoS value of 1.6 indicates the average number of carboxymethyl groups per glucopyranose unit in the polymer chain, reflecting the degree of modification. DoS suggests a substantial introduction of carboxymethyl

groups, which is corroborated by the observed changes in the FTIR spectra (Fig. 5), particularly the broadening and shifting of the O—H stretching band and the emergence of the carboxyl group stretching vibrations.

*Fourier transform infrared spectroscopy:* FTIR spectroscopy is used to analyze KGM and CMKGM to identify and confirm the presence of functional groups within the native KGM and when it is chemically modified to produce CMKGM, FTIR can detect the introduction of new functional groups, indicating successful carboxymethylation. This comparative analysis between KGM and CMKGM using FTIR is crucial for ensuring the intended chemical changes. The FTIR spectrum of KGM and CMKGM are presented in Fig. 5. These FTIR results were consistent with the previous studies done [38]. In KGM, the O—H group stretching
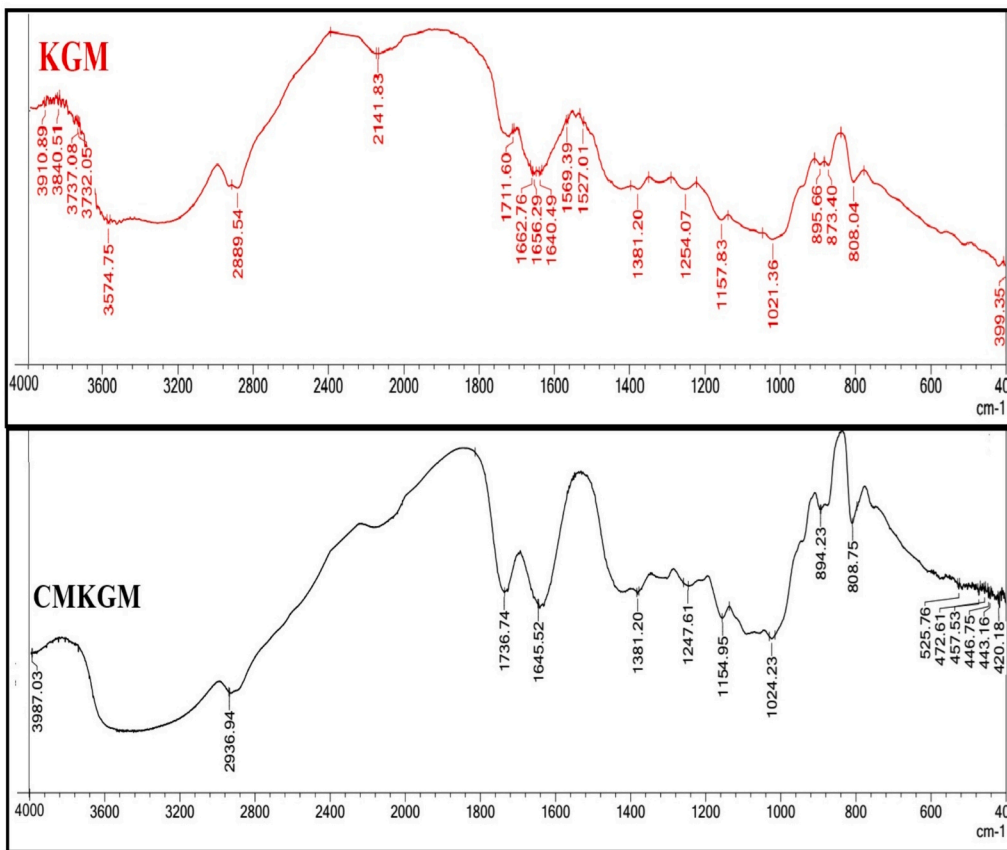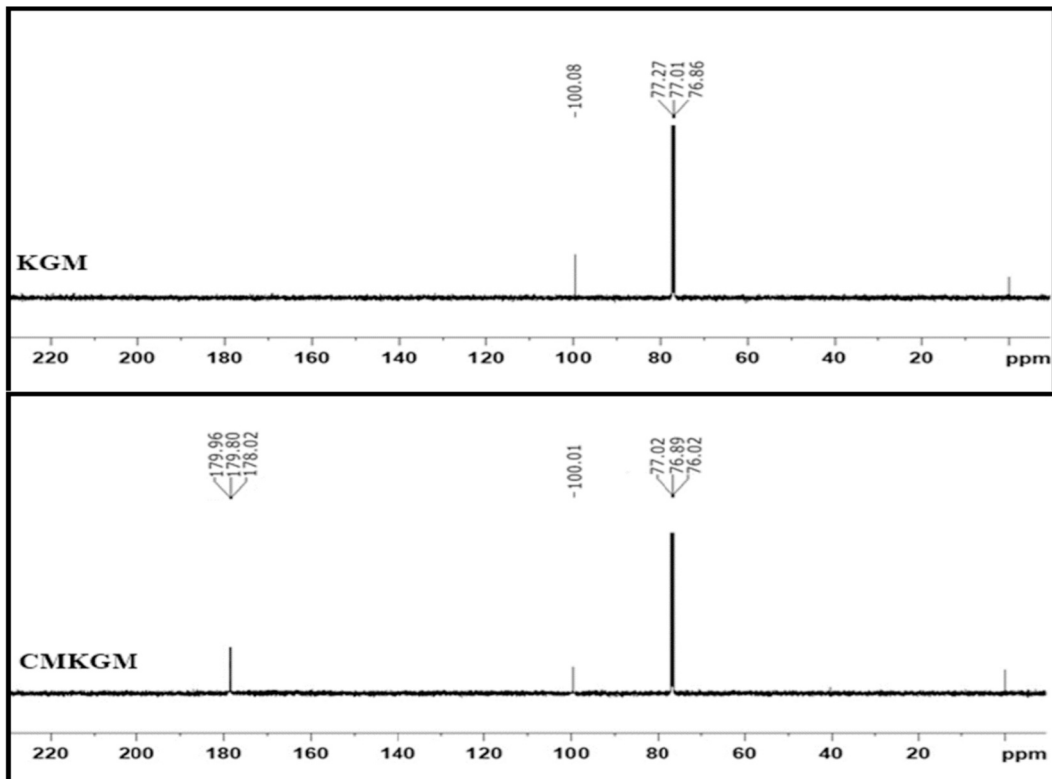
**Fig. 5.** FTIR spectra of KGM and CMKGM.



**Fig. 6.** $^{13}C$ NMR Spectra of KGM and CMKGM.

vibrations were identified as the source of the broad band observed in the 3574.75–3910.89 cm$^{-1}$ region [39]. The broadening of this band in the FTIR spectra of CMKGM suggests that carboxymethylation has altered the hydrogen bonding patterns of hydroxyl groups (-OH) in KGM. This change in intensity and broadness indicates modifications induced by the introduction of carboxymethyl groups, affecting the interactions and structural characteristics of the polymer. Similar broadening of peaks has been observed in studies where native starches were modified [40] and β-D-glucan, isolated from *Poria cocos*, was carboxymethylated [41] to enhance their characteristics. This phenomenon underscores a common trend in polysaccharide modification, where the introduction of carboxymethyl groups alters hydrogen bonding patterns, often resulting in broader and sometimes shifted peaks in the FTIR spectra.

In KGM spectra, the peak at 2889.54 cm$^{-1}$ corresponded to the C—H stretching vibrations in the –CH$_2$ or –CH$_3$ groups and at 1711.60 cm$^{-1}$ reflects the stretching vibration of the carbonyl group. Wang et al., reported this as a characteristic acetyl group of KGM molecules [42]. In native KGM, the absorption bands at 1662.76, 1656.29, and 1640.49 cm$^{-1}$ indicate the presence of intra-molecular hydrogen bonding in native KGM [43]. These bands are characteristic of the interactions between hydroxyl groups and other functional groups within the polymer, stabilizing its structure. Upon carboxymethylation, these bands vanished; instead, one sharp band was evidently observed at 1645.52 cm$^{-1}$. The disappearance of the band suggests that the carboxymethylation process introduces carboxymethyl groups (–CH$_2$COOH) to the polymer, which disrupts the existing intra-molecular hydrogen bonding network [44,45]. Similar peaks were observed after carboxymethylation of polysaccharide from *Cyclocarya paliurus* [46] *and Craterellus cornucopioides* [47] Similar changes were also reported by Wang et al., [48] indicating significant structural modifications in KGM upon carboxymethylation. Peaks observed between 808.04 cm$^{-1}$ and 895.66 cm$^{-1}$ indicate β-glycosidic linkages which are common in glucomannan.

Overall, the disappearance of the absorption band associated with intramolecular hydrogen bonding in native KGM, and the emergence of new bands, indicative of carboxyl group stretching vibrations, confirm the successful introduction of carboxymethyl groups into KGM [44,49]. This transformation suggests significant structural changes in CMKGM compared to its native counterpart.

*$^{13}$C NMR Spectroscopy:* The $^{13}$C NMR results provide detailed structural information about CMKGM (Fig. 6). By carefully analyzing the $^{13}$C NMR spectra, we can confirm the presence of carboxymethyl groups on the KGM backbone. In the $^{13}$C NMR spectra of unmodified KGM, distinct signals are observed in the range of 76.76, 77.01 and 77.27 ppm. These signals are associated with the carbon atoms of the glucopyranose ring, which is the primary structural unit of KGM. Specifically, these chemical shifts correspond to the C2, C3, and C5 carbons within the glucopyranose units, which are characteristic of the polysaccharide structure of KGM. The signal appeared at 110.08 ppm and typically corresponds to the carbon atoms in the anomeric positions of the glucose units within the polymer structure. The appearance of this peak confirms the presence of glycosidic bonds within the KGM molecule, specifically indicating the carbon environment of the anomeric carbons in the glucose units [50]. Upon carboxymethylation, significant changes are noted in the $^{13}$C NMR spectra of CMKGM. New signals emerged at of 179.96, 179.80 and 178.02 ppm. These new peaks indicate the presence of carboxyl carbon atoms (C=O) from the carboxymethyl groups that have been introduced into the polymer backbone. These peaks represent the carbon atoms directly bonded to the carboxylate groups (COO$^-$) of the carboxymethyl groups introduced onto the KGM backbone. Similar results were observed in the $^{13}$C NMR spectra after carboxymethylation of chitosan [51]. The slight variations in the signals likely correspond to different neighboring environments or conformations of the carboxymethyl groups within the polymer structure. These peaks were absent in the $^{13}$C NMR spectra of KGM, indicating specific modifications achieved through carboxymethylation. In the $^{13}$C NMR spectra of CMKGM
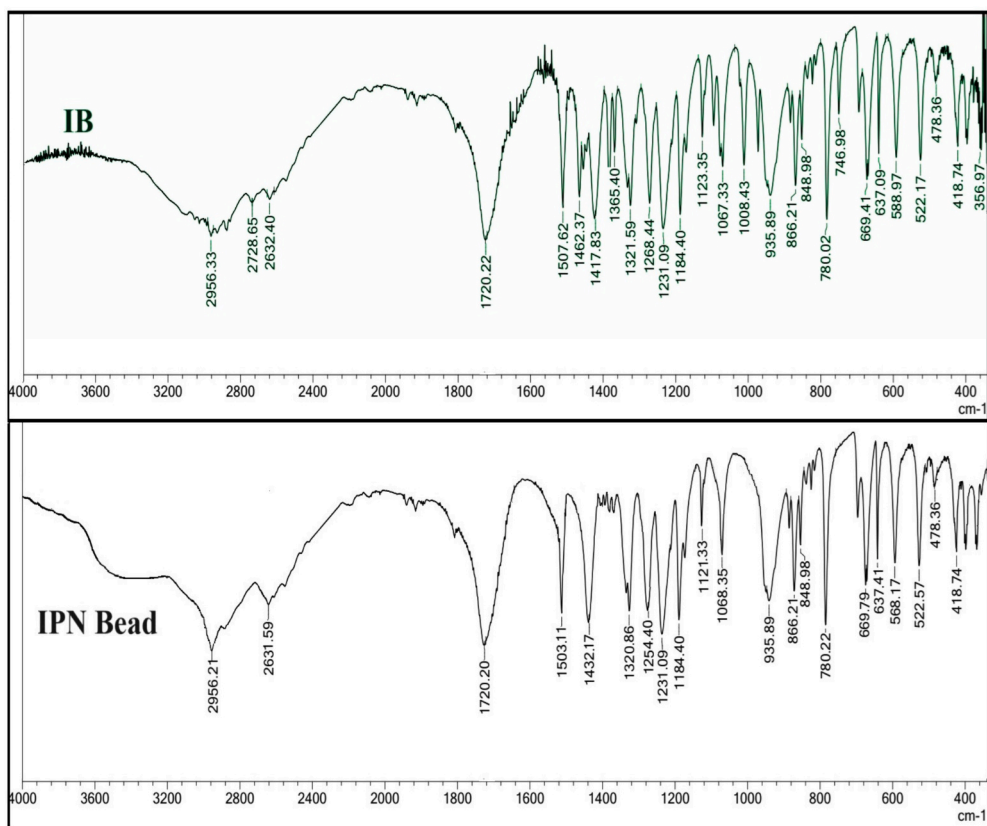


**Fig. 7.** FTIR Spectra of ibuprofen and IB-loaded IPN bead.

the signals in the range of 76–77 ppm were shifted to the down-field, this might be due to the electron-withdrawing effect of the carboxymethyl substituents. Similar downshifting of signals was reported by An NT et al. [52] The appearance of new signals specific to the carboxymethyl groups in the $^{13}$C NMR spectra of CMKGM confirms that the modification process has been successful.

### 3.2. Characterization of IPN beads

#### 3.2.1. FTIR spectroscopy

Interpreting the FTIR spectrum of IB, and beads provides valuable insights into its molecular structure, functional groups and compatibility between drugs and polymers. IB exhibits characteristic peaks in its FTIR spectrum that correspond to specific vibrational modes of its constituent atoms and functional groups. The FTIR spectrum of IB and IB-loaded IPN beads are illustrated in Fig. 7. The peak appeared at 2956.33 cm$^{-1}$ and is assigned to C—H stretching vibrations, typical of alkane groups in the molecule. The carbonyl group (C=O) of IB's carboxylic acid appears prominently as a sharp peak around 1720.22 cm$^{-1}$, indicating the presence of this functional group [53]. Peak around 1231.09 cm$^{-1}$ corresponds to the C—O stretching vibration characteristic of ester groups present in the structure of ibuprofen. Peaks from 1365.40 to 1462.37 cm$^{-1}$ are due to the C—H bending vibrations of the alkyl groups (isobutyl group) in ibuprofen. The peak at 1507.62 is indicative of C=C stretching vibrations in the aromatic ring. The presence of the benzene ring was indicated by the detection of smaller peaks within the 1268.44–1123.35 cm$^{-1}$ range. The peaks at 780.02 cm$^{-1}$ and 746.98 cm$^{-1}$ in the FTIR spectrum can be assigned to specific out-of-plane bending vibrations of the aromatic C—H bonds. The characteristic bands of IB were observed at almost similar positions in FTIR spectra of IB-loaded IPN beads, *i.e.* at 2956.21 cm$^{-1}$ and 1720.20 cm$^{-1}$, albeit with slight negligible shifts. The FTIR spectrum of IB-loaded IPN beads
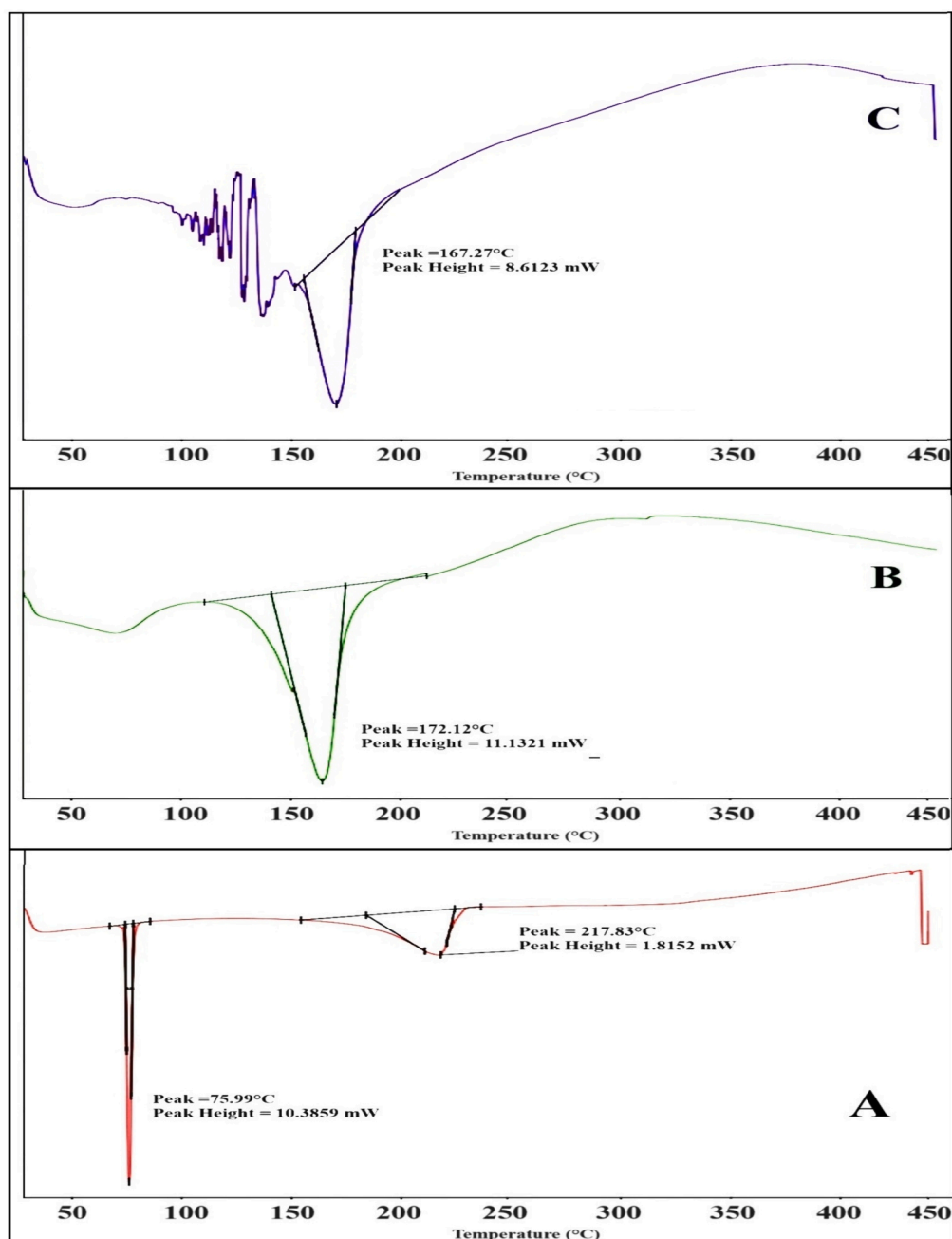


**Fig. 8.** DSC Thermogram of IB (A); Placebo IPN Bead (B); IB loaded IPN Beads (C).

exhibits all characteristic peaks of IB, confirming the absence of incompatibility between polymers and IB. This validates the successful encapsulation of IB within the beads.

### 3.2.2. Differential scanning calorimeter (DSC) study

DSC is a powerful tool for understanding the thermal characteristics and properties of the materials, making it invaluable in both research and industrial settings. It quantifies the heat flow related to transitions in materials concerning temperature variations. The use of DSC analysis is to ascertain the melting point, monitor crystalline alterations, and detect any potential incompatibility between the drug and other excipients [54].

DSC analysis of pure IB, blank and IB-loaded IPN beads (F6) were shown in Fig. 8.

In the DSC thermogram of the pure IB (Fig. 8A), a distinct sharp endothermic peak was observed and noted at 75.99 °C, which is characteristic of ibuprofen. This intense endothermic peak indicates the crystalline structure of the drug [55]. Additionally, the absence of any other significant peaks suggests the purity of the IB sample analyzed. Conversely, in DSC thermogram, IB displayed a peak within the temperature range of 184.09–224.28 °C, corresponding to its decomposition, which is expected due to the thermal instability of the compound at higher temperatures. In contrast, the DSC thermogram of the blank IPN beads (Fig. 8B) reveals endothermic peaks at approximately 172.12 °C. These peaks likely signify the removal of water molecules from the hydrogel matrix blend during the heating process. The absence of any other notable peaks suggests the thermal stability of the blank IPN beads under the experimental conditions.

The thermal analysis results of the IB-loaded beads (Fig. 8C) provide crucial insights into the behavior of the drug within the polymeric matrix. An endothermic peak at 167.27 °C was visible in the DSC thermogram of the IB-loaded beads. This peak suggests a change in the thermal behavior of the system upon drug loading. Interestingly, a slight decrease in the melting temperature of the drug is observed in the DSC thermogram of the IB-loaded IPN beads (F6) compared to pure IB. This phenomenon suggests that the presence of the polymeric matrix may influence the melting behavior of the drug, possibly due to encapsulation or dispersion within the matrix. Of significant note is the absence of the standard peak of the pure drug in the DSC thermogram of the drug-loaded IPN beads. This observation indicates uniform dispersion of the drug within the polymeric matrix, suggesting efficient incorporation of the drug into the formulation without significant aggregation or crystallization. Moreover, the DSC thermogram did not show an exothermic peak, suggesting that the IPN beads have higher thermal stability than the native polymers [36].

### 3.2.3. X-ray diffraction (XRD) study

XRD is a valuable non-destructive technique essential for understanding the crystalline characteristics of materials. It offers insights into phases, structures, preferred crystal orientations (texture), as well as various structural parameters including crystallinity, strain, crystal defects and average grain size [56]. To confirm the physical state of IB within the IPN beads, XRD studies were performed on the pure IB, empty IPN beads, and IB-containing IPN beads (F6), as shown in Fig. 9. The XRD analysis revealed sharp peaks in the X-ray diffraction patterns of IB (Fig. 9A), indicative of its crystalline nature. The characteristic XRD pattern displayed distinct peaks at 2θ values of 6.09, 13.93, 16.56, 17.59, 20.09, 22.26, and 25.0. Nevertheless, for both drug-loaded and blank hydrogel beads, these peak intensities were noticeably weak (Fig. 9B). Consequently, there was no discernible evidence of the drug's crystalline nature in the case of drug-loaded IPN hydrogel beads (Fig. 9C).

Overall, the XRD analysis confirms the successful incorporation of IB into the IPN beads and provides compelling evidence for the molecular-level dispersion of the drug within the polymer matrix. This observation is consistent with the DSC study results and further supports the

conclusion of molecular-level dispersion of IB within the polymer matrix.

### 3.3. IPN bead size analysis

The size of beads ranged from 580 ± 0.56 to 324 ± 0.27 μm, as outlined in Table 3. It was revealed that the crosslinker concentration and polymer ratio both affected the IPN bead size. The increase in SCMC content within the polymer blend corresponded with an observed enlargement in IPN bead size. This phenomenon can be elucidated through the hydrodynamic viscosity principle. According to this concept, augmenting the amount of SCMC in the CMKGM:SCMC ratio elevates the viscosity of the polymer blend within the droplets. Consequently, fewer sites are accessible for crosslinking, leading to an expansion in the size of the IPN beads [57]. The concentration of AlCl$_3$ exhibited a comparable impact on IPN bead size. As the concentration of crosslinker increased, there was a reduction in the IPN bead size. This phenomenon can be elucidated by the interaction between the blended polymer gel and the aluminium ions (Al$^{+++}$) found in the crosslinking solution. Upon contact, there is a migration of aluminium ions (Al$^{+++}$) from the crosslinker solution into the interior of the droplets, accompanied by the outward movement of water from the droplets into the surrounding solution [19]. This process causes the gel layer to contract inward. With an increase in crosslinking concentration, there is a heightened influx of aluminium ions (Al$^{+++}$) into the droplets, leading to a greater expulsion of water and subsequent contraction of the beads, resulting in a decrease in the bead size.

### 3.4. Determination of percentage yield

The study presented in Table 3 displayed the yield of IB-loaded IPN beads, indicating a percentage yield range of 95.24 % to 85.24 %. The effect of polymer ratio on the production yield of beads is a critical aspect to consider in the fabrication process. Generally, the polymer ratio refers to the relative proportions of different polymers in the blend used to form the beads. Understanding how variations in this ratio impact bead yield is essential for optimizing the manufacturing process and ensuring consistent production. Higher yields were observed with an increased amount of CMKGM in the polymer blend. However, the analysis suggests that variations in polymer ratio and crosslinker concentration did not notably influence the yield of IPN beads.

### 3.5. Determination of drug encapsulation efficiency

The drug encapsulation efficiency (DEE) of beads containing IB fell within the range of 95.42 ± 0.92 to 74.82 ± 0.12, as depicted in Table 3. The influence of both variables, ratio of CMKGM and SCMC and concentration of crosslinker, on the encapsulation efficiency of IB was clearly evident. The efficiency of drug encapsulation decreased as the amount of SCMC in the polymer ratio (CMKGM: SCMC) was increased. This phenomenon may be explained by the higher solubility of SCMC, which leads to the creation of a less dense polymer matrix and consequent enlargement of the IPN beads [58]. This less dense matrix is less effective at trapping the IB molecules. Increased bead swelling during gelation in the crosslinker solution causes IB particles to escape the interpenetrating polymer matrix, reducing the encapsulation of IB. On the other hand, it was demonstrated that a higher amount of CMKGM in the polymer ratio is associated with higher encapsulation efficiency. Increasing the amount of CMKGM in the polymer blend results in a denser, less swollen, and more stable polymer matrix. This tighter network restricts the movement of IB molecules, preventing them from diffusing out of the matrix and thereby increasing the encapsulation efficiency. It was demonstrated that as the crosslinker concentration rose, drug entrapment efficiency rose as well [59]. Higher concentrations of AlCl$_3$ lead to more extensive crosslinking within the polymer matrix. This results in a denser and more tightly bound network that
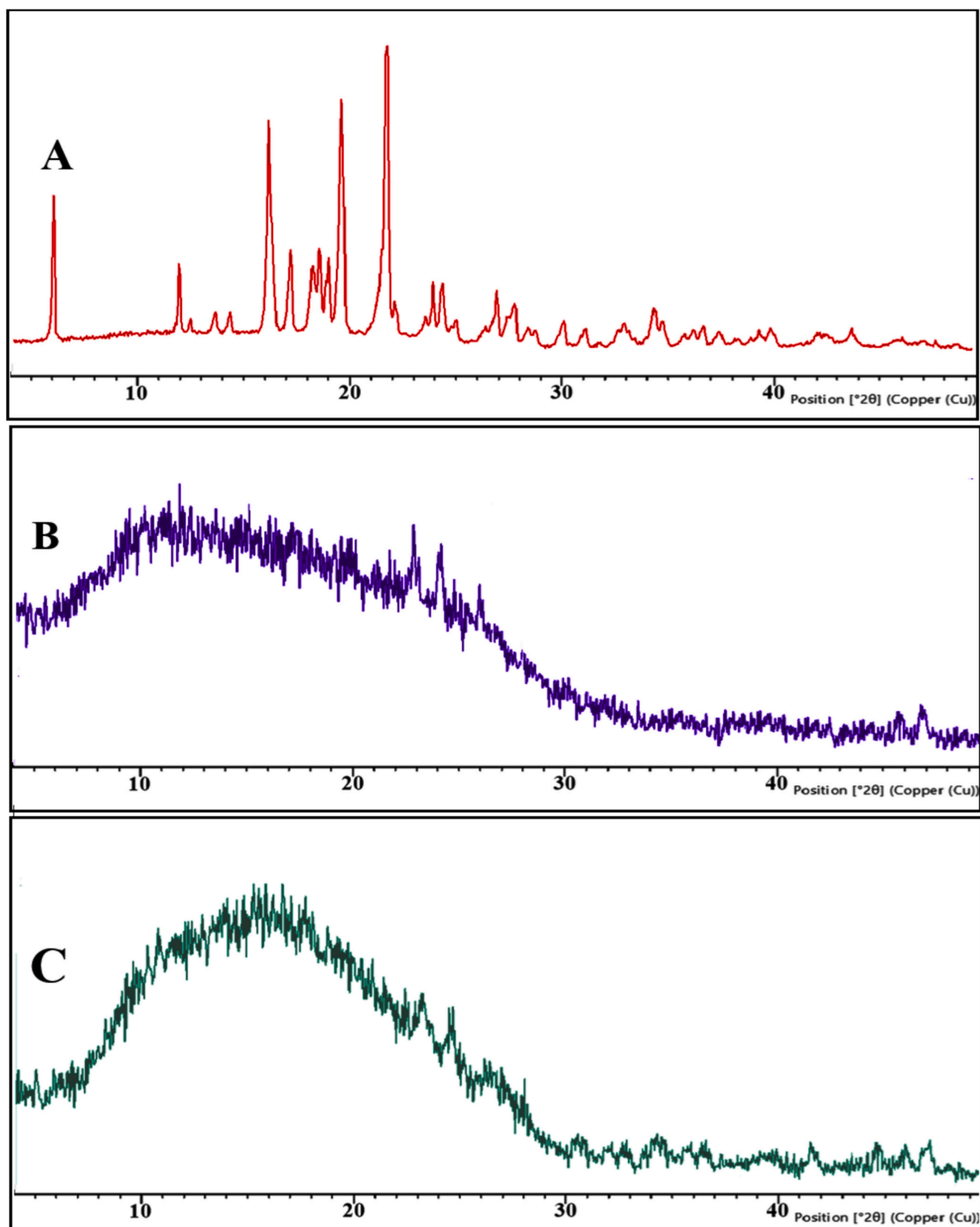
**Fig. 9.** X-ray diffractogram of -IB (A); empty IPN beads (B); IB loaded beads-F6 (C).

**Table 3**

Percentage yield, arithmetic mean diameter and drug encapsulation efficiency of prepared bead formulations.

| Formulation code | Percentage yield (%) | Bead size [Arithmetic mean diameter] (µm) ± SD | Drug encapsulation efficiency (%) |
|---|---|---|---|
| $F_1$ | 90.04 | 520 ± 0.12 | 80.80 ± 0.45 |
| $F_2$ | 92.60 | 492 ± 0.14 | 84.30 ± 0.56 |
| $F_3$ | 85.24 | 420 ± 0.12 | 88.08 ± 0.82 |
| $F_4$ | 90.36 | 550 ± 0.23 | 78.56 ± 0.95 |
| $F_5$ | 89.28 | 580 ± 0.56 | 74.82 ± 0.12 |
| $F_6$ | 94.20 | 430 ± 0.84 | 86.68 ± 0.80 |
| $F_7$ | 94.28 | 394 ± 0.22 | 89.06 ± 0.45 |
| $F_8$ | 95.24 | 324 ± 0.27 | 95.42 ± 0.92 |
| $F_9$ | 90.33 | 456 ± 0.14 | 82.68 ± 0.55 |
| $F_{10}$ | 90.62 | 482 ± 0.20 | 80.62 ± 0.42 |

effectively traps the drug molecules.

### 3.6. Swelling response to different pH

To evaluate the pH sensitivity, we examined the swelling ability of the IPN beads. The swelling data are presented in Table 4, highlighting the behavior of beads under different pH conditions—specifically, pH 1.2, 3.0, 6.8, 7.4 and 9.0. The prepared IPN beads demonstrated clear pH-responsive behavior. In acidic conditions (pH 1.2 and 3.0), the swelling capacity of the beads was significantly lower compared to that in pH 6.8 and 7.4. This behavior can be attributed to the ionizable carboxylic groups (-COOH) present in the polymer network. In acidic environments, these carboxylic groups remain largely protonated, resulting in negligible electrostatic repulsion between polymer chains. Consequently, this leads to minimal swelling. At pH 1.2, the swelling percentages range from 152.25 % (F6) to 210.22 % (F5). The swelling percentages increase slightly, ranging from 162.48 % (F7) to 320.26 % (F5) at pH 3.0. at pH 7.4 the swelling percentages continue to increase, ranging from 299.12 % (F6) to 589.86 % (F5). At physiological pH, the swelling behavior peaks for many formulations. Conversely, in alkaline environments, the carboxylic groups ionize (deprotonate), increasing the electrostatic repulsion within the polymer network. This repulsion causes the network to expand, thereby increasing the swelling of the IPN beads [60]. Similar repulsion or swelling behavior was observed by carboxymethyl chitosan hydrogel in an alkaline medium [61]. Our findings indicate that the swelling capacity of IPN beads is inversely related to the concentration of the crosslinker. Beads prepared with lower crosslinker concentrations exhibited greater swelling. Specifically, as the crosslinker concentration was increased from 2 % (*w/v*) to 4 % (w/v), the swelling capacity decreased. Similar results were reported by authors who used genipine or $CaCl_2$ as a crosslinker. Ibrahim et al. found that the swelling percentage of $CaCl_2$-crosslinked alginate-CMC beads was high at low crosslinker concentrations. However, as

the concentration of crosslinker increased, the swelling percentage of the beads decreased [62]. Du et al., reported similar effects with genipine crosslinked chitosan membranes [63]. This inverse relationship can be explained by the denser network structure formed at higher crosslinker concentrations, which restricts the movement of polymer chains and limits the ability of the network to absorb water [63].

Furthermore, the study revealed that beads with higher SCMC content exhibited greater swelling compared to those with lower SCMC content. This increased swelling can be attributed to the higher availability of functional groups, such as -COOH and -OH, in SCMC. These groups facilitate hydrogen bonding with water molecules, enhancing the hydration and expansion of the polymer network. Therefore, IPN beads with higher SCMC content have a more pronounced response to pH changes due to the increased number of ionizable groups contributing to the swelling behavior. Similar effects were observed by Varaprasad et al., where they have reported that a high concentration of SCMC shows a higher swelling ratio of semi-IPN hydrogel prepared from SCMC-based Poly(acrylamide-*co*-2acrylamido-2-methyl-1-propane sulfonic acid) [57].

At pH 9.0, the swelling behavior of IPN beads shows marked differences among various formulations, with some formulations attaining high swelling percentages, leading to the dissolution of the beads (F4, F5, F9, F10). The swelling behavior at pH 9 reveals the critical interplay between crosslinker concentration and SCMC content in determining the structural stability of IPN beads. Formulations with lower crosslinker concentrations and higher SCMC content (F4, F5) exhibit excessive swelling due to the increased availability of functional groups for hydrogen bonding and ionization at alkaline pH. This leads to substantial osmotic pressure and, ultimately, the dissolution of beads when the crosslinking is insufficient to counterbalance the expansion forces. This pH condition is particularly challenging for maintaining the structural integrity of the beads due to the enhanced deprotonation of functional groups and increased osmotic pressure. The pH-responsive swelling behavior of these IPN beads suggests their potential utility in controlled drug delivery applications. In acidic environments, such as the stomach, the minimal swelling would result in a slower release of the encapsulated drug. Conversely, in the more alkaline environment (pH 7.4) of the intestines, the increased swelling would facilitate a faster release of the drug, ensuring that it is available for absorption at the appropriate site within the gastrointestinal tract.

### 3.7. Surface morphology/SEM analysis

The scanning electron microscopy (SEM) results presented in Fig. 10 illustrate the influence of altering $AlCl_3$ concentrations on the size and surface morphology of the IPN beads. Observations reveal that as the concentration of crosslinker (Al+++) increases, the IPN beads tend to adopt a more spherical shape. Specifically, a comparison between Formulation F-6, containing a 4 % *w/v* solution of crosslinker, and

**Table 4**

Percentage Equilibrium swelling of IPN Beads.

| Formulation Code | Percentage Equilibrium swelling of IPN Beads (%) ± SD | | | | |
|---|---|---|---|---|---|
| | pH 1.2 | pH 3.0 | pH 6.8 | pH 7.4 | pH 9.0 |
| $F_1$ | 160.20 ± 1.60 | 172.60 ± 1.20 | 220.45 ± 0.95 | 338.10 ± 1.52* | 396.76 ± 2.02 |
| $F_2$ | 162.42 ± 1.62 | 170.45 ± 1.30 | 288.62 ± 0.98 | 392.62 ± 1.95* | 408.23 ± 1.96 |
| $F_3$ | 180.56 ± 1.24 | 195.62 ± 1.06 | 310.68 ± 1.02 | 428.44 ± 1.98* | 450.78 ± 1.63 |
| $F_4$ | 185.06 ± 1.22 | 204.63 ± 1.0 | 350.64 ± 0.98 | 499.05 ± 2.10* | 596.24 ± 1.22 (at 12th hr, after that beads were dissolved) |
| $F_5$ | 210.22 ± 1.42 | 320.26 ± 0.98 | 482.62 ± 0.99 | 589.86 ± 1.86* | 586.24 ± 2.20 (at 10th hr, after that beads were dissolved) |
| $F_6$ | 152.25 ± 1.49 | 164.02 ± 0.14 | 198.62 ± 1.93 | 299.12 ± 1.88* | 308.03 ± 2.36 |
| $F_7$ | 158.24 ± 1.02 | 162.48 ± 1.02 | 210.66 ± 1.25 | 374.26 ± 1.84* | 352.62 ± 1.99 |
| $F_8$ | 169.23 ± 1.26 | 174.62 ± 1.04 | 228.15 ± 0.99 | 382.60 ± 1.64* | 386.46 ± 1.02 |
| $F_9$ | 174.30 ± 1.65 | 186.42 ± 1.0 | 312.69 ± 0.62 | 456.23 ± 1.96* | 526.24 ± 1.56 (at 18th hr, after that beads were dissolved) |
| $F_{10}$ | 192.03 ± 1.25 | 216.63 ± 1.62 | 332.45 ± 0.88 | 498.62 ± 1.96* | 556.24 ± 1.89 (at 16th hr, after that beads were dissolved) |

* Means $p < 0,05$: there is a statistically significant difference between the values of the samples at pH 1.2 and pH 7.4 (independent samples *t*-test).
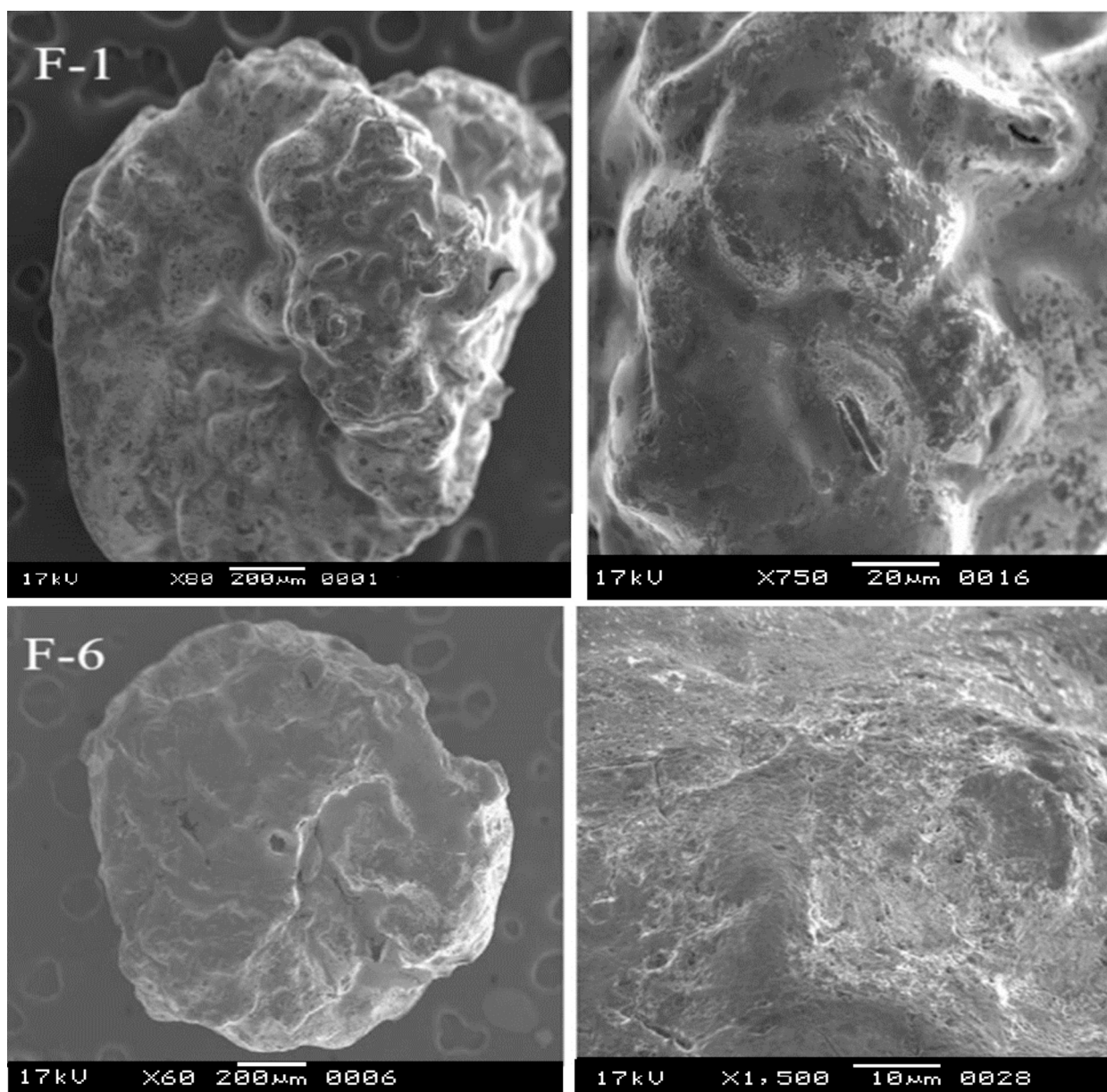
**Fig. 10.** SEM image of IB-loaded IPN beads (comparison of effect of concentration of crosslinker- AlCl$_3$). F1 (2 % *w/v*), F6 (4 % w/v), other formulation composition is same.

Formulation F-1, containing a 2 % w/v solution, highlights this trend. The beads within Formulation F-6 exhibit a notably spherical morphology, whereas those in Formulation F-1 appear rough with discernible wrinkles on the surface. These findings indicate a correlation between crosslinker concentration and the resultant morphology of the IPN beads, with higher concentrations leading to enhanced spherical shapes.

The impact of the polymer ratio (CMKGM: SCMC) on the surface morphology of IPN beads is demonstrated in Fig. 11. Notably, at higher concentrations of CMKGM, the surface of the beads appeared remarkably smooth, accompanied by a more spherical bead shape. This can be attributed to several key factors. Firstly, the higher probability of CMKGM molecules interacting and entangling in the polymer matrix at elevated concentrations leads to the formation of a more cohesive network structure within the bead matrix. This enhanced polymer interaction contributes to improved bead cohesion and structural integrity, thereby facilitating the development of smoother surfaces and more uniform shapes [64]. Additionally, the increased concentration of CMKGM promotes more efficient crosslinking during the curing process, strengthening the intermolecular bonds between polymer chains and resulting in a more compact and uniform bead structure. Overall, these combined effects underscore the sensitivity of bead morphology to variations in CMKGM concentration. Conversely, when the concentration of SCMC was elevated, the surface of the beads exhibited pronounced roughness, with visible cracks and wrinkles. SCMC is a hydrophilic polymer with a high water absorption capacity. At higher concentrations, SCMC may absorb more water during the bead formation process, leading to increased swelling and distortion of the polymer matrix [44]. This swelling can contribute to the formation of surface wrinkles and roughness as the beads dry or cure. These observations highlight the sensitivity of IPN bead morphology to variations in polymer ratio, with differing concentrations of CMKGM and SCMC yielding distinct surface characteristics and shapes.
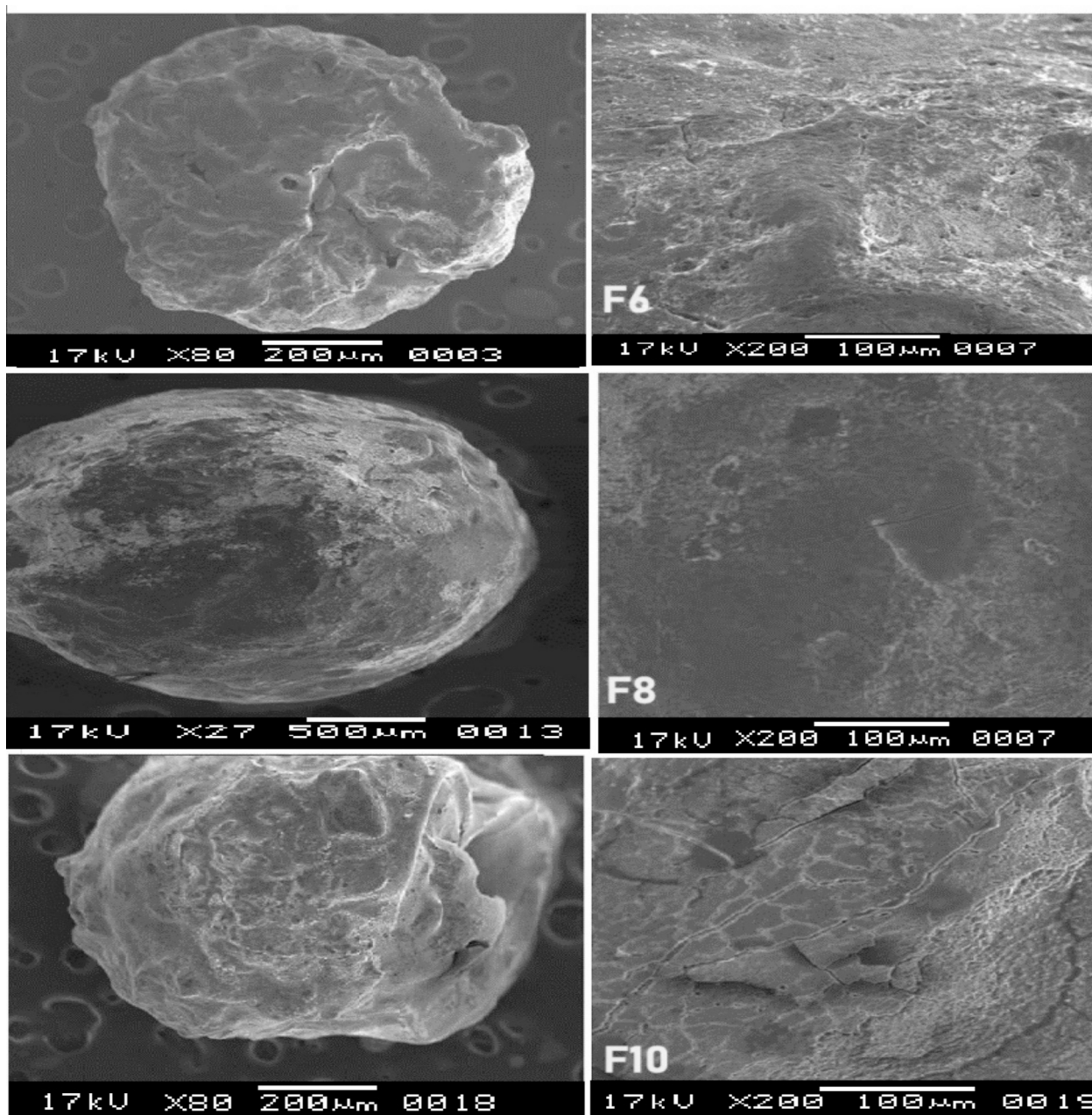
**Fig. 11.** SEM image of IB-loaded IPN beads (comparison of effect of polymer ratio CMKGM:SCMC). F6 (1:1), F8 (2:1) and F10 (1:2).

### 3.8. In vitro drug release study

The human gastrointestinal tract presents varying pH conditions as a drug travels from the acidic stomach to the more alkaline small intestine. IB-loaded IPN beads were employed to examine the release of IB. The initial 2 h of the experiment were conducted in an acidic (pH 1.2) environment, followed by the subsequent phase in an alkaline (pH 7.4) environment. By studying the release over 2 h in pH 1.2, we simulate the early stages of drug dissolution and release in the stomach after oral administration. This period is crucial as it reflects the immediate release behavior of the drug under acidic conditions, which is relevant for drugs designed to be rapidly absorbed. Following oral administration, the first 2 h in pH 1.2 typically correspond to the time when a significant portion of the gastric emptying occurs post-meal ingestion. This timeframe is chosen to capture the initial release profile that directly affects drug absorption kinetics in the body. After the initial gastric phase, transitioning to pH 7.4 (simulating intestinal conditions) allows us to

observe how the formulation behaves in a less acidic, more alkaline environment. This phase is important for understanding sustained release patterns and drug availability beyond the immediate absorption phase. Fig. 12 depicts the relationship between the cumulative percent of drug release and time (hrs). The results show that in acidic conditions, there is little release of IB from IPN beads; nevertheless, as the media's pH increases to 7.4, there is a notable increase in IB release from IPN beads. The lower cumulative drug release percentage of IB-loaded beads observed in acidic pH could be attributed to the restricted swelling capacity of the beads under acidic conditions [65]. The disparity in drug release between IPN beads with low concentration (2 %*w/v*) and those with a higher crosslinker concentration (4 %*w/v*) can be attributed to the differing degrees of polymer network rigidization [35]. Specifically, the heightened crosslinker concentration induces greater rigidity within the polymer network, thereby slowing down the release of IB. As a result, IPN beads with a lower crosslinker concentration exhibit a higher rate of drug release compared to their counterparts with a higher
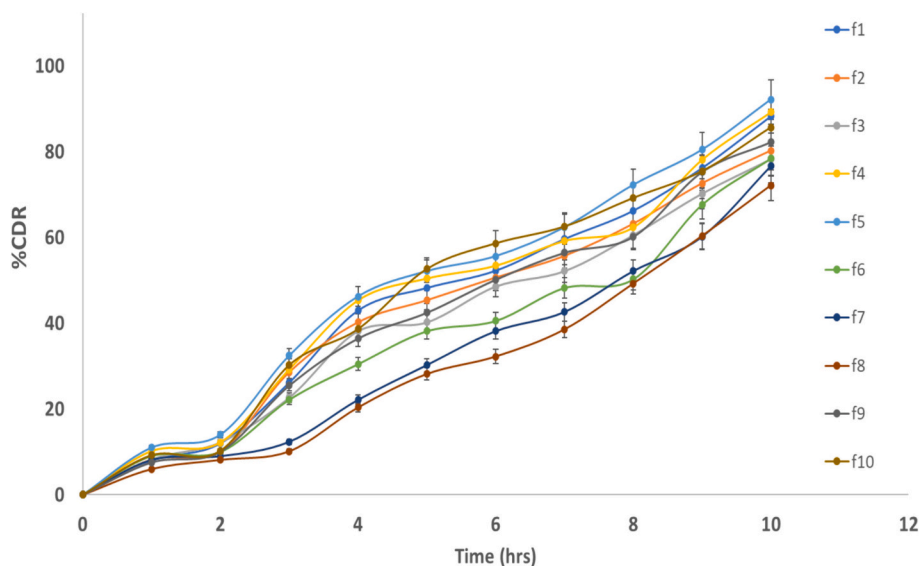
**Fig. 12.** Cumulative drug release percentage of IB-loaded IPN beads in gastric media (pH = 1.2 for initial 2 h) and intestinal media (pH = 7.4).

**Table 5**
Release mechanism and kinetic modelling of drug release data.

| Formulation | Zero order | First order | Higuchi | Korsmeyer–Peppas | |
|---|---|---|---|---|---|
| | $r^2$ | $r^2$ | $r^2$ | $r^2$ | N |
| $F_1$ | 0.9836 | 0.9035 | 0.9156 | 0.9704 | 0.879 |
| $F_2$ | 0.9766 | 0.9556 | 0.9180 | 0.8974 | 0.891 |
| $F_3$ | 0.9800 | 0.9467 | 0.9044 | 0.8767 | 0.918 |
| $F_4$ | 0.9662 | 0.8748 | 0.9091 | 0.9013 | 0.971 |
| $F_5$ | 0.9741 | 0.8796 | 0.9179 | 0.8764 | 0.985 |
| $F_6$ | 0.9767 | 0.8876 | 0.8804 | 0.9555 | 0.861 |
| $F_7$ | 0.9713 | 0.8720 | 0.8339 | 0.9350 | 0.956 |
| $F_8$ | 0.9649 | 0.8815 | 0.8152 | 0.9476 | 0.856 |
| $F_9$ | 0.9884 | 0.9318 | 0.9083 | 0.9666 | 0.925 |
| $F_{10}$ | 0.9761 | 0.9557 | 0.9237 | 0.9395 | 0.902 |

concentration of crosslinker.

The regression coefficient approach was used to analyze the data, and Table 5 shows the regression coefficient values ($r^2$) for the IPN bead formulations. A zero-order release pattern was found when the release kinetics of IB from IPN bead compositions were examined. This suggests that the rate of drug release remains constant over time, irrespective of the concentration of IB. The application of the Korsmeyer-Peppas release kinetics and mechanism equation yielded "n" values (0.9649 to 0.9884), indicating a super case-II release mechanism characterized by sorption controlled by stress-induced relaxations within swellable polymer matrix systems. In such system, the swelling of the polymer matrix under the influence of external factors, such as hydration or changes in environmental conditions, triggers stress-induced relaxations within the polymer matrix structure.

## 4. Conclusion

Polymers serve as essential components in the advancement of novel drug delivery systems, owing to their adjustable characteristics, biocompatibility, and capacity to manage drug release kinetics. Carboxymethylation of polymers stands out as a versatile and efficient technique for crafting controlled drug delivery systems endowed with customized release profiles, heightened solubility, and augmented biocompatibility. This method holds considerable promise across diverse pharmaceutical applications. Additionally, IPNs emerge as a novel category of polymers, amalgamating natural and synthetic polymers either independently or in amalgamations. IPNs offer a platform

for designing drug delivery systems with tailored properties, combining the favorable attributes of different polymers to achieve enhanced performance and functionality. Their utilization holds significant potential in various pharmaceutical realms, contributing to the development of advanced and effective therapeutic interventions.

The carboxymethylation of KGM was successfully conducted, followed by the development of IPN beads utilizing CMKGM, SCMC, and AlCl$_3$. These IPN beads served as carriers for oral delivery of encapsulated IB. Comprehensive characterization of the IB-loaded IPN beads was performed using SEM, FTIR, XRD, and DSC. The results of FTIR confirmed the stability of IB within the IPN. The results demonstrated how the concentration of the crosslinking agent and the polymer ratio significantly affect several factors, including bead size, drug encapsulation, bead swelling, and drug release characteristics. DSC results revealed that the IPN beads exhibit greater thermal stability compared to the native polymers. The data obtained from the XRD analysis indicates that IB is dispersed or scattered at the molecular level inside the polymer matrix. The IPN beads size ranged from 580 ± 0.56 to 324 ± 0.27 μm with nearly spherical morphology. Additionally, the drug release behavior of the IPN beads showed a significant and prolonged release profile in alkaline circumstances, but negligible drug release in acidic medium. These findings suggest the potential utility of IB-loaded IPN beads in attenuating drug release in acidic environments and modulating drug release in alkaline conditions, thereby mitigating potential gastric adverse effects associated with IB administration, making this system particularly advantageous for oral delivery.

**CRediT authorship contribution statement**

**Alka Lohani:** Writing – review & editing, Writing – original draft, Supervision, Methodology, Investigation, Conceptualization. **Ritika Saxena:** Writing – original draft, Methodology, Investigation, Conceptualization. **Shahbaz Khan:** Writing – original draft, Methodology, Investigation, Conceptualization. **Filipa Mascarenhas-Melo:** Writing – review & editing, Writing – original draft, Supervision, Conceptualization.

**Declaration of competing interest**

The authors declare that they have no known competing financial interests or personal relationships that could have appeared to influence the work reported in this paper.

# References

[1] O. Pillai, R. Panchagnula, Polymers in drug delivery, Curr. Opin. Chem. Biol. 5 (4) (2001) 447–451.

[2] T.C. Ezike, U.S. Okpala, U.L. Onoja, P.C. Nwike, E.C. Ezeako, J.O. Okpara, C. C. Okoroafor, S.C. Eze, O.L. Kalu, E.C. Odoh, U. Nwadike, Advances in drug delivery systems, challenges and future directions, Heliyon 9 (6) (2023) 17488.

[3] S. Grund, M. Bauer, D. Fischer, Polymers in drug delivery—state of the art and future trends, Adv. Eng. Mater. 13 (3) (2011) 61–87.

[4] M.B. Ashford, R.M. England, N. Akhtar, Highway to success—developing advanced polymer therapeutics, Adv. Ther. 4 (5) (2021) 200–285.

[5] P. Bhatt, S. Trehan, N. Inamdar, V.K. Mourya, A. Misra, Polymers in drug delivery: an update, in: Applications of Polymers in Drug Delivery, 2nd edition, Elsevier, 2021, pp. 1–42.

[6] I. Benalaya, G. Alves, J. Lopes, L.R. Silva, A review of natural polysaccharides: sources, characteristics, properties, food, and pharmaceutical applications, Int. J. Mol. Sci. 25 (2024) 1322.

[7] M. Baghel, K. Sakure, T.K. Giri, S. Maiti, K.T. Nakhate, S. Ojha, C. Sharma, Y. Agrawal, S. Goyal, H. Badwaik, Carboxymethylated gums and derivatization: strategies and significance in drug delivery and tissue engineering, Pharmaceuticals 16 (5) (2023) 776.

[8] V. Rana, S. Kamboj, R. Sharma, K. Singh, Modification of gums: synthesis techniques and pharmaceutical benefits, in: Handbook of Polymers for Pharmaceutical Technologies: Biodegradable Polymers 28, 2015, pp. 299–364.

[9] A. Lohani, G. Singh, S.S. Bhattacharya, A. Verma, Interpenetrating polymer networks as innovative drug delivery systems, J. Drug Del. (2014) 583612.

[10] C. Roy, A. Gandhi, S. Manna, S. Jana, Fabrication and evaluation of carboxymethyl guar gum-chitosan interpenetrating polymer network (IPN) for controlled drug delivery, Med. Novel Technol. Devices. 22 (2024 Jun 1) 100300.

[11] S.S. Behera, R.C. Ray, Konjac glucomannan, a promising polysaccharide of Amorphophallus konjac K. Koch in health care, Int. J. Biol. Macromol. 1 (92) (2016) 942–956.

[12] Y. Sun, X. Xu, Q. Zhang, D. Zhang, X. Xie, H. Zhou, Z. Wu, R. Liu, J. Pang, Review of konjac glucomannan structure, properties, gelation mechanism, and application in medical biology, Polymers 15 (8) (2023) 1852.

[13] Y.H. Mao, Y.X. Xu, Y.H. Li, J. Cao, F.L. Song, D. Zhao, Y. Zhao, Z.M. Wang, Y. Yang, Effects of konjac glucomannan with different molecular weights on gut microflora with antibiotic perturbance in in vitro fecal fermentation, Carbohydr. Polym. 273 (2021) 118546.

[14] L.H. Wang, G.Q. Huang, T.C. Xu, J.X. Xiao, Characterization of carboxymethylated konjac glucomannan for potential application in colon-targeted delivery, Food Hydrocoll. 94 (2019) 354–362.

[15] V.P. Chakka, T. Zhou, Carboxymethylation of polysaccharides: synthesis and bioactivities, Int. J. Biol. Macromol. 165 (2020) 2425–2431.

[16] E. Chikhaoui, E. Cherif, E. Herth, Chitosan and sodium carboxymethylcellulose biocomplex interaction properties for biomedical and pharmaceutical applications, Phase Transit. 97 (3) (2024) 212–227.

[17] A.K. Bajpai, S.K. Shukla, Water sorption and mechanical properties of binary polymeric blends of polyvinyl alcohol and sodium carboxymethyl cellulose, J. Macromol. Sci., Part A: Pure Appl. Chem. 41 (1) (2004) 45–62.

[18] R.K. Madhusudana, B. Mallikarjuna, K.S. Krishna Rao, M.N. Prabhakar, K. Chowdoji Rao, M.C. Subha, Preparation and characterization of pH sensitive poly (vinyl alcohol)/sodium carboxymethyl cellulose IPN microspheres for in vitro release studies of an anti-cancer drug, Polym. Bull. 68 (2012) 1905–1919.

[19] V. Ramesh Babu, K.S. Krishna Rao, M. Sairam, B.V. Naidu, K.M. Hosamani, T. M. Aminabhavi, pH sensitive interpenetrating network microgels of sodium alginate-acrylic acid for the controlled release of ibuprofen, J. Appl. Polym. Sci. 99 (5) (2006) 2671–2678.

[20] E. Bulut, Development and optimization of Fe3+-crosslinked sodium alginate-methylcellulose semi-interpenetrating polymer network beads for controlled release of ibuprofen, Int. J. Biol. Macromol. 168 (2021) 823–833.

[21] B. Arıca, S. Çalış, P. Atilla, N.T. Durlu, N. Çakar, H.S. Kaş, A.A. Hıncal, In vitro and in vivo studies of ibuprofen-loaded biodegradable, alginate beads, J. Microencapsul. 22 (2005) 153–165.

[22] L. Li, J. Zhao, Y. Sun, F. Yu, J. Ma, Ionically cross-linked sodium alginate/ κ-carrageenan double-network gel beads with low-swelling, enhanced mechanical properties, and excellent adsorption performance, Chem. Eng. J. 15 (372) (2019) 1091–1103.

[23] M. Rani, A. Agarwal, T. Maharana, Y.S. Negi, A comparative study for interpenetrating polymeric network (IPN) of chitosan-amino acid beads for controlled drug release, Afr. J. Pharm. Pharmacol. 4 (2) (2010) 35–54.

[24] Q. Xu, W. Huang, L. Jiang, Z. Lei, X. Li, H. Deng, KGM and PMAA based pH-sensitive interpenetrating polymer network hydrogel for controlled drug release, Carbohydr. Polym. 97 (2) (2013) 565–570.

[25] N. Orakdogen, Novel responsive poly (N, N-dimethylaminoethyl methacrylate) gel beads: preparation, mechanical properties and pH-dependent swelling behavior, J. Polym. Res. 19 (2012) 1–10.

[26] M. Prabaharan, J.F. Mano, Stimuli-responsive hydrogels based on polysaccharides incorporated with thermo-responsive polymers as novel biomaterials, Macromol. Biosci. 6 (12) (2006) 991–1008.

[27] J. Khan, A. Alexander, Ajazuddin, S. Saraf, S. Saraf, Biomedical applications of interpenetrating polymer network gels, in: Interpenetrating Polymer Network: Biomedical Applications, 2020, pp. 289–312.

[28] K. Mallikarjuna Reddy, V. Ramesh Babu, K.S. Krishna Rao, M.C. Subha, K. Chowdoji Rao, M. Sairam, T.M. Aminabhavi, Temperature sensitive semi-IPN microspheres from sodium alginate and N-isopropylacrylamide for controlled release of 5-fluorouracil, J. Appl. Polym. Sci. 107 (5) (2008 Mar 5) 2820–2829.

[29] S.B. Park, J.O. You, H.Y. Park, S.J. Haam, W.S. Kim, A novel pH-sensitive membrane from chitosan—TEOS IPN; preparation and its drug permeation characteristics, Biomaterials 22 (4) (2001 Feb 15) 323–330.

[30] M. Zeng, Z. Fang, Preparation of sub-micrometer porous membrane from chitosan/polyethylene glycol semi-IPN, J. Membr. Sci. 245 (1–2) (2004 Dec 1) 95–102.

[31] B.R. Sharma, V. Kumar, P.L. Soni, P. Sharma, Carboxymethylation of Cassia tora gum, J. Appl. Polym. Sci. 12 (2003) 3216–3219.

[32] D.A. Silva, R.C. De Paula, J.P. Feitosa, A.C. De Brito, J.S. Maciel, H.C. Paula, Carboxymethylation of cashew tree exudate polysaccharide, Carbohydr. Polym. 58 (2) (2004 Nov 19) 163–171.

[33] Y. Tezuka, Y. Tsuchiya, T. Shiomi, 13C NMR determination of substituent distribution in carboxymethylcellulose by use of its peresterified derivatives, Carbohydr. Res. 291 (1996 Sep 23) 99–108.

[34] A. Lohani, M. Maurya, S. Kumar, N. Verma, IPN beads prepared by tailoring of cassia tora gum and sodium carboxymethyl cellulose using $Al^{+++}$ for controlled drug delivery, J. Drug Deliv. Sci. Technol. 81 (2023) 104–308.

[35] S.S. Bhattacharya, S. Shukla, S. Banerjee, P. Chowdhury, P. Chakraborty, A. Ghosh, Tailored IPN hydrogel bead of sodium carboxymethyl cellulose and sodium carboxymethyl xanthan gum for controlled delivery of diclofenac sodium, Polym.-Plast. Technol. Eng. 52 (8) (2013) 795–805.

[36] J. Ayarza, Y. Coello, J. Nakamatsu, SEM–EDS study of ionically cross-linked alginate and alginic acid bead formation, Int. J. Polym. Anal. Charact. 22 (1) (2017) 1–10.

[37] X.L. Liu, C.F. Zhu, H.C. Liu, J.M. Zhu, Quantitative analysis of degree of substitution/molar substitution of etherified polysaccharide derivatives, Des. Monomers Polym. 25 (1) (2022) 75–88.

[38] C. Wu, Y. Li, Y. Du, L. Wang, C. Tong, Y. Hu, J. Pang, Z. Yan, Preparation and characterization of konjac glucomannan-based bionanocomposite film for active food packaging, Food Hydrocoll. 1 (89) (2019) 682–690.

[39] T. Hong, J.Y. Yin, S.P. Nie, M.Y. Xie, Applications of infrared spectroscopy in polysaccharide structural analysis: progress, challenge and perspective, Food Chem. X. 30 (12) (2021) 100–168.

[40] I. Ali, M. Ahmad, S. Ridha, C.C. Iferobia, N. Lashari, Dual modification approach for tapioca starch using gamma irradiation and carboxymethylation, Hybrid. Adv. 1 (3) (2023) 100071.

[41] Y. Wang, Y. Xu, Y. Chen, Surface modification on polyurethanes by using bioactive carboxymethylated fungal glucan from *Poria cocos*, Colloids Surf. B Biointerfaces 1; 81 (2) (2010) 629–633.

[42] L.X. Wang, A.R. Lee, Y. Yuan, X.M. Wang, T.J. Lu, Preparation and FTIR, Raman and SEM characterizations of konjac glucomannan-KCl electrogels, Food Chem. 30 (331) (2020) 127289.

[43] K. Wang, Z. He, Alginate–konjac glucomannan–chitosan beads as controlled release matrix, Int. J. Pharm. 244 (1) (2002) 117–126.

[44] J. Du, R. Sun, S. Zhang, T. Govender, L.F. Zhang, C.D. Xiong, et al., Novel polyelectrolyte carboxymethyl konjac glucomannan–chitosan nanoparticles for drug delivery, Macromol. Rapid Commun. 25 (9) (2004) 954–958.

[45] Y. An, H. Liu, X. Li, J. Liu, L. Chen, X. Jin, T. Chen, W. Wang, Z. Liu, M. Zhang, F. Liu, Carboxymethylation modification, characterization, antioxidant activity and anti-UVC ability of Sargassum fusiforme polysaccharide, Carbohydr. Res. 1 (515) (2022) 108555.

[46] Z.J. Wang, J.H. Xie, M.Y. Shen, W. Tang, H. Wang, S.P. Nie, M.Y. Xie, Carboxymethylation of polysaccharide from Cyclocarya paliurus and their characterization and antioxidant properties evaluation, Carbohydr. Polym. 20 (136) (2016) 988–994.

[47] Y. Liu, X. Duan, M. Zhang, C. Li, Z. Zhang, B. Hu, A. Liu, Q. Li, H. Chen, Z. Tang, W. Wu, Extraction, structure characterization, carboxymethylation and antioxidant activity of acidic polysaccharides from Craterellus cornucopioides, Ind. Crop. Prod. 159 (2021) 113079.

[48] L.H. Wang, G.Q. Huang, T.C. Xu, J.X. Xiao, Characterization of carboxymethylated konjac glucomannan for potential application in colon-targeted delivery, Food Hydrocoll. 1 (94) (2019) 354–362.

[49] J. Du, J. Dai, J.L. Liu, T. Dankovich, Novel pH-sensitive polyelectrolyte carboxymethyl Konjac glucomannan-chitosan beads as drug carriers, React. Funct. Polym. 66 (10) (2006) 1055–1061.

[50] N.T. An, N.T. Dong, P. Le Dung, N. Van Du, Characterization of glucomannan from some Amorphophallus species in Vietnam, Carbohydr. Polym. 25;80 (1) (2010) 308–311.

[51] L. Chen, Y. Du, X. Zeng, Relationships between the molecular structure and moisture-absorption and moisture-retention abilities of carboxymethyl chitosan: II. Effect of degree of deacetylation and carboxymethylation, Carbohydr. Res. 7;338 (4) (2003) 333–340.

[52] N.T. An, N.T. Dong, P. Le Dung, Synthesis and characterization of water-soluble O-carboxymethyl glucomannan derivatives, Carbohydr. Polym. 10;83 (2) (2011) 645–652.

[53] S.R. Matkovic, G.M. Valle, L.E. Briand, Quantitative analysis of ibuprofen in pharmaceutical formulations through FTIR spectroscopy, Lat. Am. Appl. Res. 35 (3) (2005) 189–195.

[54] R. Chadha, S. Bhandari, Drug–excipient compatibility screening—role of thermoanalytical and spectroscopic techniques, J. Pharm. Biomed. Anal. 87 (2014) 82–97.

[55] A. Wahab, G.M. Khan, M. Akhlaq, N.R. Khan, A. Hussain, A. Zeb, A. Rehman, K. U. Shah, Pre-formulation investigation and in vitro evaluation of directly compressed ibuprofen-ethocel oral controlled release matrix tablets: a kinetic approach, Afr. J. Pharm. Pharmacol 5 (19) (2011) 2118–2127.

[56] A.A. Bunaciu, E.G. UdriŞTioiu, H.Y. Aboul-Enein, X-ray diffraction: instrumentation and applications, Crit. Rev. Anal. Chem. 45 (4) (2015) 289–299.

[57] K. Varaprasad, K. Vimala, S. Ravindra, N.N. Reddy, K.M. Raju, Development of sodium carboxymethyl cellulose-based poly (acrylamide-co-2acrylamido-2-methyl-1-propane sulfonic acid) hydrogels for in vitro drug release studies of ranitidine hydrochloride an anti-ulcer drug, Polym.-Plast. Technol. Eng. 50 (12) (2011) 1199–1207.

[58] C. Chittasupho, J. Angklomklew, T. Thongnopkoon, W. Senavongse, P. Jantrawut, W. Ruksiriwanich, Biopolymer hydrogel scaffolds containing doxorubicin as a localized drug delivery system for inhibiting lung cancer cell proliferation, Polymers 13 (20) (2021) 3580.

[59] S. Mitra, S. Maity, B. Sa, Effect of different cross-linking methods and processing parameters on drug release from hydrogel beads, Int. J. Biol. Macromol. 74 (2015) 489–497.

[60] M. Zhang, X.H. Li, Y.D. Gong, N.M. Zhao, X.F. Zhang, Properties and biocompatibility of chitosan films modified by blending with PEG, Biomaterials 23 (13) (2002) 2641–2648.

[61] Y. Luo, Z. Teng, X. Wang, Q. Wang, Development of carboxymethyl chitosan hydrogel beads in alcohol-aqueous binary solvent for nutrient delivery applications, Food Hydrocoll. 31 (2) (2013) 332–339.

[62] S.M. Ibrahim, F.I. Abou El Fadl, A. El-Naggar, Preparation and characterization of crosslinked alginate–CMCbeads for controlled release of nitrate salt, J. Radioanal. Nucl. Chem. 299 (2014) 1531–1537.

[63] J.R. Du, L.H. Hsu, E.S. Xiao, X. Guo, Y. Zhang, X. Feng, Using genipin as a "green" crosslinker to fabricate chitosan membranes for pervaporative dehydration of isopropanol, Sep. Purif. Technol. 244 (2020) 116843.

[64] N.A. Ibrahim, B.W. Chieng, W.M.Z. Wan Yunus, Morphology, thermal and mechanical properties of biodegradable poly (butylenes succinate)-poly (butylene adipate-co-terephthalate)-clay nanocomposites, Polym.-Plast. Technol. Mater. 49 (2010) 1571–1580.

[65] Y. Li, R. Fan, H. Xing, Y. Fei, J. Cheng, L. Lu, Study on swelling and drug releasing behaviors of ibuprofen-loaded bimetallic alginate aerogel beads with pH-responsive performance, Colloids Surf. B Biointerfaces 205 (2021) 111–895.